IOPscience iopscience.iop.org

Home Search Collections Journals About Contact us My IOPscience

Stress and Defect Distribution of Thick GaN Film Homoepitaxially Regrown on Free-Standing GaN by Hydride Vapor Phase Epitaxy

This content has been downloaded from IOPscience. Please scroll down to see the full text.

2010 Jpn. J. Appl. Phys. 49 091001

(http://iopscience.iop.org/1347-4065/49/9R/091001)

View the table of contents for this issue, or go to the journal homepage for more

Download details:

IP Address: 140.113.38.11
This content was downloaded on 25/04/2014 at 06:05

Please note that terms and conditions apply.

Stress and Defect Distribution of Thick GaN Film Homoepitaxially Regrown on Free-Standing GaN by Hydride Vapor Phase Epitaxy

Kuei-Ming Chen[1,2*], Yen-Hsien Yeh[1], Yin-Hao Wu[1], Chen-Hao Chiang[1], Din-Ru Yang[1], Zhong-Shan Gao[1], Chu-Li Chao[1,2], Tung-Wei Chi[2], Yen-Hsang Fang[2], Jenq-Dar Tsay[2], and Wei-I Lee[1]

[1] *Department of Electrophysics, National Chiao Tung University, Hsinchu 300, Taiwan*
[2] *Electronics and Optoelectronics Research Laboratories, Industrial Technology Research Institute, Hsinchu 300, Taiwan*

Received October 1, 2009; accepted June 21, 2010; published online September 21, 2010

A 220-μm-thick Gallium nitride (GaN) layer was homoepitaxially regrown on the Ga-polar face of a 200-μm-thick free-standing *c*-plane GaN by hydride vapor-phase epitaxy (HVPE). The boundary of the biaxial stress distribution in the GaN substrate after regrowth was clearly distinguished. One half part, the regrown GaN, was found to be more compressive than the other half part, the free-standing GaN. Additionally, the densities of the screw and mixed dislocations reduced from 2.4×10^7 to 6×10^6 cm^{-2} after regrowth. Furthermore, the yellow band emission almost disappeared, accompanied by a peak emission at approximately 380 nm related to the edge dislocation was under slightly improved in regrown GaN. We conclude that the reduction of the dislocation defects and Ga vacancies and/or O impurities are the two main reasons for the higher compressive stress in the regrown GaN than in the free-standing GaN, causing the curvature of the GaN substrate to be twice concave after regrowth. © 2010 The Japan Society of Applied Physics

DOI: 10.1143/JJAP.49.091001

1. Introduction

Gallium nitride (GaN) is the most suitable substrate for manufacturing high-performance nitride-based devices, e.g., short-wavelength light-emitting diodes (LEDs),[1] laser diodes (LD),[2] high electron mobility transistors (HEMTs),[3] and rectifiers,[4] owing to the homogeneity of its lattice constant and its thermal expansion coefficient (TEC) when it is overgrown with device epitaxial layers.[5] The several methods developed for manufacturing GaN substrates include high pressure growth,[6] Na flux,[7] ammonothermal growth,[8] and hydride vapor-phase epitaxy (HVPE).[9] The most used commercially method for fabricating a thick GaN film is HVPE by depositing a GaN epilayer on a foreign base substrate, e.g., sapphire, Si, SiC, GaAs, or $LiAlO_2$, with a high growth rate and reliability. The many approaches developed to separate GaN thick films from the original substrates and produce free-standing GaN include chemical etching,[10] self-separation,[11] and laser lift-off (LLO).[12] For epilayer growth to form various devices, the surface of free-standing GaN substrates is polished to improve the uniformity and decrease surface roughness.[13] However, the parasitic deposition of GaN in an HVPE reactor and TECs between GaN and the foreign base substrate mainly limit the growth of a sufficiently thick and crack-free GaN to support polishing.[14,15] Tsai *et al.* were the first to use HVPE to regrow GaN on free-standing GaN, as obtained by LLO, to improve its thickness and quality.[16] Lucznik *et al.* adopted free-standing GaN with a low dislocation density, as produced using high N2 pressure, as a starting substrate to regrow GaN by HVPE.[17] Darakchieva *et al.* observed that the strain in the homoepitaxial GaN layer increased slightly with respect to the freestanding GaN. Additionally, the strain could be attributed to an interfacial defective region between the free-standing and the homoepitaxial GaN.[18] However, the relationship before and after regrowth between the stress and crystalline quality and bowing has not been investigated. Using the HVPE system, in this study, we elucidate the homoepitaxy of regrown GaN on free-standing GaN, which is obtained by HVPE and LLO.

*E-mail address: mapu.ep96g@g2.nctu.edu.tw

2. Experimental Procedure

A 3-μm-thick undoped GaN layer was initially grown by metalorganic chemical vapor deposition (MOCVD) on *c*-plane sapphire substrates as a GaN template. The GaN thick film was then grown on a GaN template, using the temperature ramping method that was developed in our earlier study by horizontal HVPE.[19] In the growth of GaN in the HVPE reactor, NH_3 and GaCl were generated from liquid gallium and HCl gas at 850 °C, as sources of nitrogen and gallium, respectively. The pressure was maintained at 700 Torr, and a mixture of H_2 and N_2 was applied as the carrier gas. The thickness of GaN in this first step of HVPE growth was 200 μm, and the corresponding growth rate was about 100 μm/h. After it was cooled to room temperature, the 200-μm-thick GaN film with a 1 in. diameter was separated from the sapphire substrate using the LLO method with a 355 nm Nd:YAG laser. Next, the Ga residue at the N-polar face of the free-standing GaN that was formed from decomposed GaN was removed using a solution of HCl/H_2O. The Ga-polar face of the free-standing GaN was then chemically cleaned with acetone, alcohol, and deionized (DI) water. HVPE regrowth was subsequently performed on the Ga-polar face of the free-standing GaN in pure H_2 carrier gas at a temperature of 1050 °C and a pressure of 700 Torr. In the second step of HVPE growth, the 220-μm-thick regrown GaN film was deposited on the Ga-polar face of free-standing GaN, yielding a 420-μm-thick GaN substrate.

The surface and cross-sectional morphology of the HVPE GaN layers were observed under a Nomarski microscope and a scanning electronic microscope (SEM). On the basis of optical measurements, the stress and optical quality of the GaN epilayers were determined using PL at the surface plane and CL at the cross-sectional plane. Next, the stress distribution in free-standing GaN and regrown GaN was analyzed on the basis of micro-Raman and CL measurements. The PL measurement was performed with He–Cd laser excitation at 325 nm at a power of 14 mW at room temperature and 20 K with a slit width of 0.1 mm. The spatial and spectral resolutions are about 1 mm and 0.1 nm, respectively. The CL measurement was performed with accelerating voltages of 15 kV and a probing current of

 © 2010 The Japan Society of Applied Physics

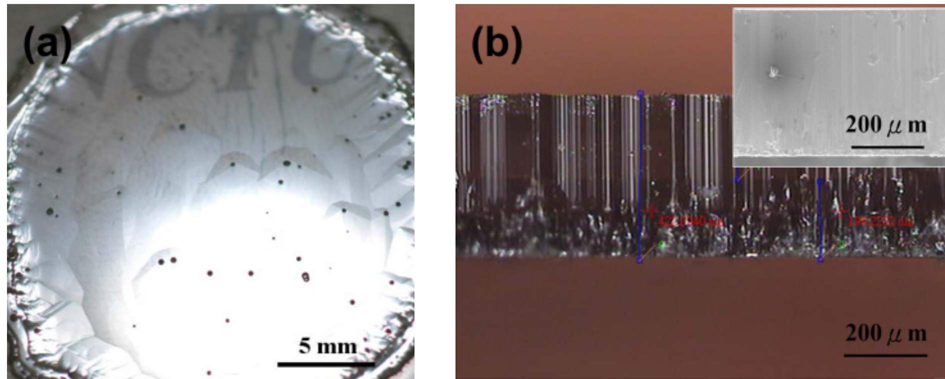

Fig. 1. (Color online) (a) Digital camera image taken using flash of the 1 in. 420-μm-thick crack-free GaN substrate after regrowth. (b) Cross-sectional view of GaN substrate taken using Nomarski contrast. The inset is a cross-sectional SEM image of the GaN substrate.

14 nA at room temperature. The spectral resolution and slit width are about 0.02 nm and 0.2 mm, respectively. The micro-Raman measurement was performed with Ar laser excitation with a wavelength of 488 nm at a power of 5 mW at room temperature with a slit width of 0.2 mm. The spatial and spectral resolutions of the Raman setup are about 2 μm and 0.02 cm^{-1}, respectively. The sample used in the etching pit density (EPD) experiment was etched at 220 °C for 20 min in a mixed solution of H_3PO_4 and H_2SO_4 at a ratio of 1 : 3; measurements were then taken using an atomic force microscope (AFM). Moreover, the crystalline properties of the GaN epilayers were examined using high-resolution X-ray diffraction (HRXRD). Finally, the (002) and (102) diffraction peaks in the X-ray rocking curve were identified using a Bede D1 system with a Cu sealed anode.

3. Results and Discussion

Figure 1(a) displays an image, captured using a digital camera with a flash, of the crack-free GaN substrate after the second step of HVPE growth. The GaN substrate is transparent but has several pits at its irregular edge. Additionally, some huge pits are observed in the central region of the GaN substrate, pits that often appear on the top of huge and flat hillocks. Such pits are present in free-standing GaN before regrowth, and increase in size during regrowth owing to the stability of the hexagonal plane. Figure 1(b) presents a cross-sectional Nomarski contrast image of the GaN substrate. The interface between free-standing GaN (~200 μm, in the lower part of the figure) and regrown GaN (~220 μm, in the upper part of the figure) can be clearly distinguished. Furthermore, the free-standing GaN is darker than the regrown GaN, because of the higher carrier concentration. However, the interface between free-standing GaN and regrown GaN in the cross-section SEM image inset in Fig. 1(b) can not be observed, indicating the continuous growth of GaN.

Figure 2 shows the variation and degree of bowing of GaN on sapphire, free-standing GaN, and the GaN substrate. The bowing radius changes from 3 m^{-1} before LLO to 0.47 m^{-1} after LLO. This reduction is attributed to the relaxation of bowing and compressive strain attributed to the TEC mismatch between GaN and sapphire when the GaN film is separated from the sapphire. However, the free-standing GaN after LLO was slightly bowed in a concave manner while the GaN on sapphire exhibited serious convex

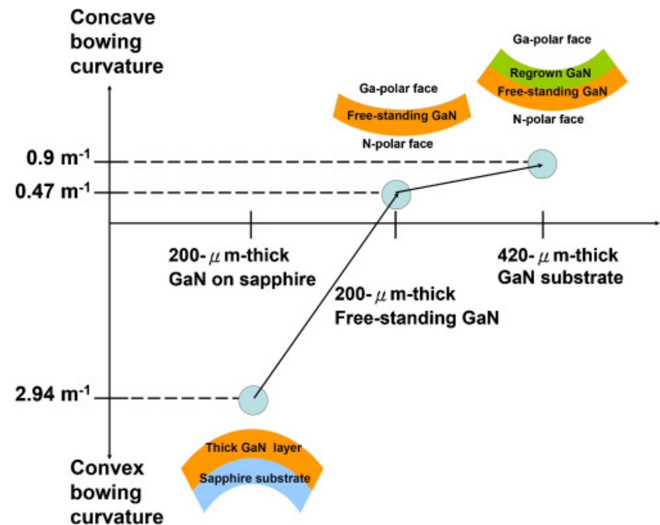

Fig. 2. (Color online) Bowing direction and curvature of thick GaN on sapphire, free-standing GaN, and the GaN substrate.

bowing, which is caused by the high density of defects at the N-polar face of the free-standing GaN following LLO.[20] After regrowth on the Ga-polar face of the free-standing GaN, the bowing radius increased from 0.47 to 0.9 m^{-1} and is also concave. This finding suggests that the bowing of GaN is more serious because of the higher quality of regrown GaN, resulting in compressive biaxial stress, than that of free-standing GaN. The following measurements describe the experimental values and origin of the stress variation.

Figure 3(a) and Table I present the PL spectrum at the Ga- and N-polar faces of free-standing GaN and GaN substrate. The near-band-edge (NBE) peak is blue-shifted from 362.8 to 362.4 nm at the Ga-polar face and is red-shifted from 363.3 to 363.7 nm at the N-polar face after regrowth. Tensile or compressive biaxial stress can be calculated with reference to the strain-free emission peak at 365 nm.[21] Although compressive biaxial stress exists at the Ga-polar face of both the free-standing GaN and the GaN substrate, the latter exhibits a greater stress. In contrast, the compressive biaxial stress existing at the N-polar face of GaN substrate is smaller than that of the N-polar face of free-standing GaN. Kisielowski *et al.* found that a biaxial stress of 1 GPa shifts the near-band-edge PL lines by 27 ±

 © 2010 The Japan Society of Applied Physics

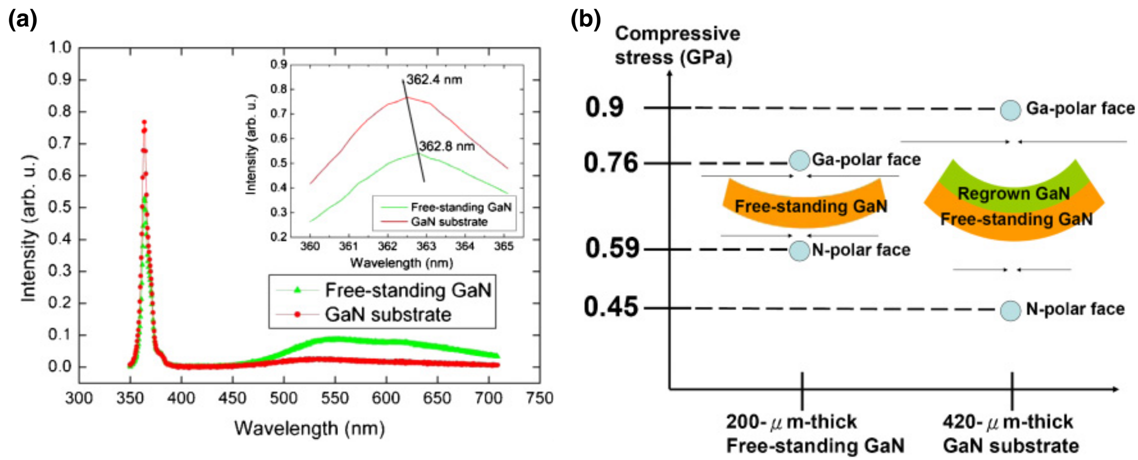

Fig. 3. (Color online) (a) PL spectrum taken at the Ga-polar face of the free-standing GaN and the GaN substrate. The inset diagram is the spectrum around the NBE. (b) Difference in compressive stress between the Ga- and N-polar faces of the free-standing GaN and the GaN substrate.

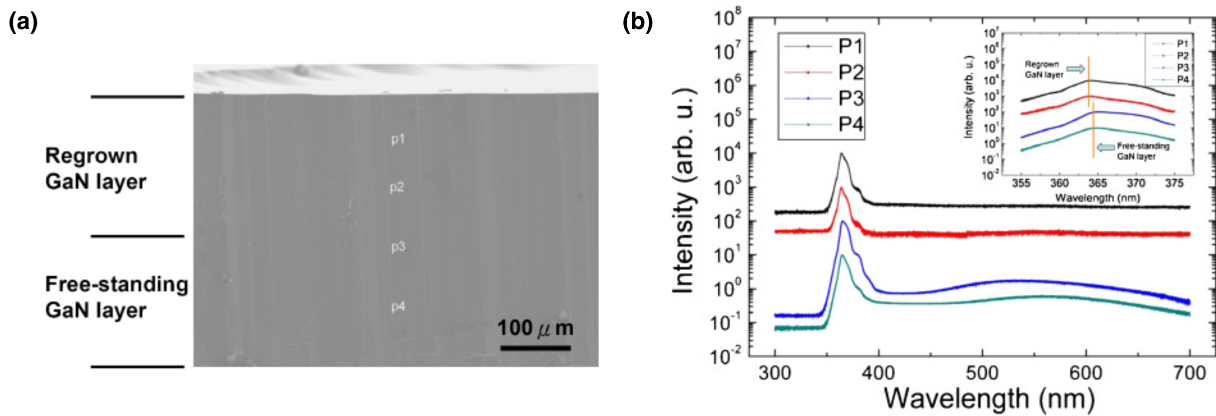

Fig. 4. (Color online) (a) SEM and (b) relative CL spectra were obtained at the crosssection of the GaN substrate after regrowth. The upper part is regrown GaN (P1 and P2, 65 and 135 μm depth from the Ga-polar face of the GaN substrate after regrowth) and the lower part is free-standing GaN (P3 and P4, 225 and 320 μm depth from the Ga-polar face of the GaN substrate after regrowth). The inset diagram is the spectrum around the NBE.

Table I. PL measurements at the Ga- and N-polar faces of the free-standing GaN and the GaN substrate.

	Free-standing GaN		GaN substrate	
	Ga-polar face	N-polar face	Ga-polar face	N-polar face
NBE peak (nm)	362.8	363.3	362.4	363.7
Compressive biaxial stress (GPa)	0.76	0.59	0.9	0.45
Difference in biaxial stress between Ga- and N-polar faces (GPa)	0.17		0.45	
FWHM (nm)	5.7	10.2	4.6	10.4

2 meV.[22] According to calculations of the wavelength of the NBE peak, the compressive biaxial stress at the Ga- and N-polar faces is 0.76 and 0.59 GPa in free-standing GaN, respectively, and 0.9 and 0.45 GPa in the GaN substrate, respectively. We believe that the concave bowing is more serious because the difference in the compressive biaxial stress between the Ga- and N-polar faces increases after regrowth, as shown in Fig. 3(b). Moreover, the FWHM at the Ga-polar face decreases from 5.7 to 4.6 nm, indicating that the defect was decreased. Additionally, after regrowth, the yellow band emission declined almost to the level of disappearance at the Ga-polar face, as shown in Fig. 3(a). This finding suggests that the concentration of Ga vacancies and/or O impurities is significantly reduced.[23] This is one of the reasons that the compressive stress is larger at the Ga-polar face in the GaN substrate than that in the free-standing GaN because the Ga vacancies and/or O impurities are related to tensile stresses. Furthermore, in this study, low-temperature PL (20 K) also formed on the Ga-polar face on the free-standing GaN and GaN substrate before and after regrowth. The intensity of donor-bound-exciton (DBE) significantly decreased after regrowth, indicating that the O impurities decreased as well.[24] Moreover, an emission peak appeared at approximately 380 nm at the Ga-polar face of both the free-standing GaN and the GaN substrate. Reshchikov and Morkoç assigned this peak to the edge dislocation defect.[24] The peak intensity, which is comparable to that associated with NBE, becomes slightly smaller after regrowth. This finding suggests that the edge dislocation is slightly improved after regrowth, as discussed later in the dislocation analysis.

This stress observation is verified in Fig. 4 by the cross-sectional CL spectrum at four depths (P1 to P4, from the Ga- to N-polar face of the GaN substrate after regrowth).

 © 2010 The Japan Society of Applied Physics

Table II. Listed data of CL and Raman measurements of different depths from the Ga-polar face of the GaN substrate after regrowth.

	P1 (65 μm)	P2 (135 μm)	P3 (225 μm)	P4 (320 μm)
CL				
NBE peak (nm)	364.2	364.1	365.2	364.9
FWHM (nm)	7.6	6.9	8.9	7.8
Raman				
E2(high) (cm^{-1})	567.830	567.886	567.774	567.774
E1(TO) (cm^{-1})	559.369	559.554	559.277	559.277
A1(TO) (cm^{-1})	531.401	531.587	531.958	531.958

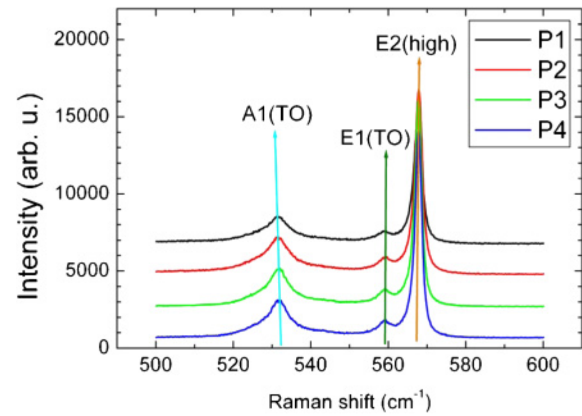

Fig. 5. (Color online) Raman spectra in the cross-sectional regions of the GaN substrate were obtained at the same positions (P1 to P4) as of the cross-sectional CL measurements in Fig. 4(b).

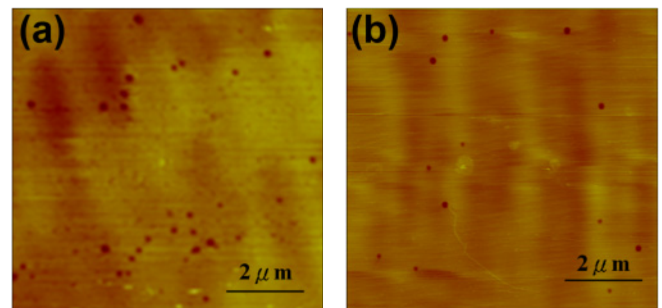

Fig. 6. (Color online) AFM image at the Ga-polar face of (a) the free-standing GaN and (b) the GaN substrate after chemical etching.

Table II presents the NBE peak position and FWHM. Interestingly, the NBE peak is clearly changed from 364 nm in the regrown (P1 and P2) to 365 nm in the free-standing (P3 and P4) parts of the GaN substrate. According to the blue-shifted NBE peak, the biaxial stress was more compressive in the regrown part of the GaN substrate. This finding further demonstrates that a large compressive biaxial stress in the upper region of the GaN substrate causes concave bowing. The wavelength of NBE is slightly larger in the cross-sectional CL measurement than that in the surface PL measurement, i.e., the corresponding stress is more tensile in the CL measurement than that in the PL measurement. We believe that it is attributed to the lack of one dimensional biaxial stress at the cross-sectional region of CL measurement. Furthermore, the difference of the biaxial stress was about 0.31 GPa between free-standing GaN and regrown GaN in cross-sectional CL measurement.[22] This is less than a quarter of 0.45 GPa in the surface PL measurement, which is due to the lack of one dimensional biaxial stress at the cross-sectional region. Moreover, the FWHM of NBE and yellow band emission are obviously lower in the regrown part of the GaN substrate, which consistent with the PL measurements. The FWHM is large at P3 (around the interface between free-standing and regrown GaN), because of damage caused by LLO and exposure to the ambient. Additionally, according to the cross-sectional CL measurements in Fig. 4(b), an emission peak of approximately 380 nm also appeared in the entire thickness. The intensity of this peak is slightly lower for the regrown part of the GaN substrate, a finding which correlates with the PL measurements.

In this study, we also elucidate the stress distribution throughout the entire thickness of the GaN substrate by obtaining Raman scattering spectra through the use of a laser light incident on the cross section presented in Fig. 5 and Table II. Three Raman active phonon peaks are clearly observed, including A1(TO) at approximately 531 cm^{-1}, E1(TO) at approximately 559 cm^{-1}, and E2(high) at approximately 567 cm^{-1}. E2(high) and E1(TO) are blue-shifted from P4 to P1, from the bottom to the top of the GaN substrate. As is well known, variation in the Raman blue-shift of these two phonon peaks indicates compressive biaxial stress.[25] The biaxial stress exhibits no variation in the entire thickness of the free-standing GaN, but becomes more compressive in the regrown GaN. The cross-sectional CL measurements also reveal this tendency. With respect to the strain free E2 (high) mode position of 567.5 cm^{-1} and the respective stresses estimated using a stress factor of 2.9 GPa/cm^{-1}, the biaxial stress was compressive in the entire thickness of the GaN substrate, which agrees with the CL measurements.[26] Moreover, the compressive stresses were 0.31 GPa at the regrown GaN part and 0.27 GPa at the free-standing GaN part. Notably, regrown GaN and free-standing GaN differed by 0.04 GPa in terms of biaxial stress, i.e., less than the difference of 0.31 GPa obtained by CL measurements. We believe that the peak shift of NBE may be attributed not only to biaxial stress, but also to origins such as dislocations, point defects, and impurities, a phenomenon also found by Darakchieva *et al.*[18] Moreover, the A1(TO) mode is related to oscillation along the *c*-axis, and the compressive biaxial stress causes tensile stress out of the plane, thereby resulting in a red-shift in the A1(TO) mode frequency.

The dislocation density before and after regrowth was also estimated based on EPD measurements at the Ga-polar face, as plotted in Fig. 6. According to this figure, the EPD decreases from 3.6×10^7 to 1.5×10^7 cm^{-2} after regrowth, providing another explanation for why the compressive stress is larger at the Ga-polar face in the GaN substrate than that in the free-standing GaN. This is because the dislocation defects are related to tensile stresses. A more detailed analysis reveals that the pits appear with different sizes before and after regrowth, as shown in Figs. 6(a) and 6(b), respectively. According to Lu *et al.*, the larger pits are related to the screw or mixed-type dislocations and the smaller ones are related to the edge-type dislocations.[27]

 © 2010 The Japan Society of Applied Physics

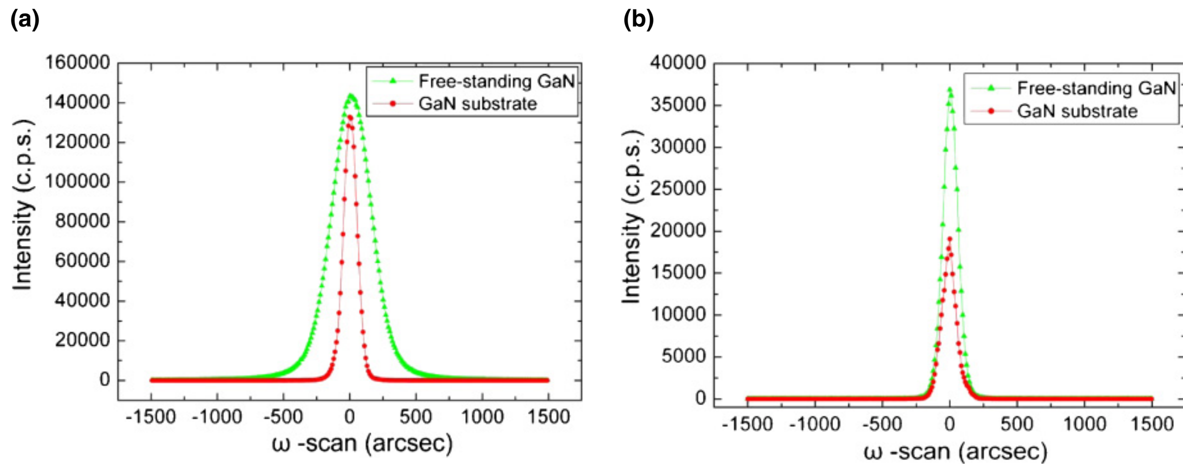

Fig. 7. (Color online) ω-scans of HRXRD in the (a) (002) and (b) (102) reflections taken before and after regrowth.

According to Figs. 6(a) and 6(b), the density of the screw or mixed dislocations fell from 2.4×10^7 to $6 \times 10^6\,\text{cm}^{-2}$, while that of the edge dislocations declined from 1.2×10^7 to $9 \times 10^6\,\text{cm}^{-2}$ after regrowth. Therefore, although the number of screw or mixed dislocations is significantly reduced, the number of edge dislocations is slightly reduced after regrowth. The latter result is consistent with the variation in the peak emission at approximately 380 nm, as revealed by the PL and CL measurements in Figs. 3 and 4(b), respectively.

Moreover, variation in the crystalline quality was confirmed on the basis of ω-scans of HRXRD in (002) and (102) reflections using a slit width of 0.5 mm, which were taken before and after regrowth. According to Fig. 7(a), the FWHM of the (002) reflection in the ω-scan was reduced from 257 to 104 arcsec after regrowth. The FWHM of the (102) reflection in the ω-scan was 113 arcsec before regrowth and 105 arcsec after regrowth, revealing no change, as shown in Fig. 7(b). According to Kappers *et al.*, the FWHM of the (002) reflection is related to the screw or mixed dislocations while the FWHM of the (102) reflection is related to the edge dislocations.[28] The bowing became more concave after regrowth enlarged FWHM in both the (002) and (102) reflections. However, despite the significant improvement in the FWHM of the (002) reflection, that of the (102) reflection remained almost unchanged after regrowth. It is attributed to the effective reduction of the screw or mixed dislocations to a quarter, the edge type dislocation only reduced to three quarters.

4. Summary

In conclusion, a 220-μm-thick GaN layer was homoepitaxially regrown on the Ga-polar face of 200-μm-thick free-standing *c*-plane GaN by HVPE. Twice the concave curvature of the GaN substrate occurred after regrowth at the Ga-polar face because the compressive biaxial stress in the regrown GaN half region exceeds that in the other free-standing GaN half region. Moreover, the difference of the compressive biaxial stress between the Ga- and N-polar faces increases after regrowth. The yellow band emission almost disappeared, indicating that the density of Ga vacancies and/or O impurities declined markedly after regrowth. The peak emission at approximately 380 nm, related to the edge dislocation defect, slightly improved. The densities of the screw and mixed dislocations were 2.4×10^7 and $6 \times 10^6\,\text{cm}^{-2}$, respectively, while that of the edge dislocations was 1.2×10^7 and $9 \times 10^6\,\text{cm}^{-2}$ before and after regrowth, respectively. We conclude that the dislocation defects and Ga vacancies and/or O impurities that were improved are the two main reasons for the more compressive biaxial stress in the regrown GaN than in the free-standing GaN, ultimately leading to the more concave bowing after regrowth. Furthermore, the FWHM of the (002) reflection of the ω-scan decreased from 257 to 104 arcsec, while that of the (102) reflection decreased from 114 to 105 arcsec after regrowth.

Acknowledgement

This study is financially supported by National Science Council of Taiwan through contract NSC 98-2221-E-009-026 and by the Ministry of Education of Taiwan, which are deeply appreciated.

1) X. A. Cao and S. D. Arthur: Appl. Phys. Lett. **85** (2004) 3971.
2) S. E. Hooper, M. Kauer, V. Bousquet, K. Johnson, C. Zellweger, and J. Heffernan: J. Cryst. Growth **278** (2005) 361.
3) M. A. Khan, J. W. Yang, W. Knap, E. Frayssinet, X. Hu, G. Simin, P. Prystawko, M. Leszczynski, I. Grzegory, S. Porowski, R. Gaska, M. S. Shur, B. Beaumont, M. Teisseire, and G. Neu: Appl. Phys. Lett. **76** (2000) 3807.
4) Y. Zhou, D. Wang, C. Ahyi, C. C. Tin, J. Williams, M. Park, N. M. Williams, and A. Hanser: Solid-State Electron. **50** (2006) 1744.
5) R. D. Vispute, V. Talyansky, S. Choopun, R. P. Sharma, T. Venkatesan, M. He, X. Tang, J. B. Halpern, M. G. Spencer, Y. X. Li, L. G. Salamanca-Riba, A. A. Iliadis, and K. A. Jones: Appl. Phys. Lett. **73** (1998) 348.
6) I. Grzegory, M. Bockowski, B. Łucznik, S. Krukowski, Z. Romanowski, M. Wroblewski, and S. Porowski: J. Cryst. Growth **246** (2002) 177.
7) M. Aoki, H. Yamane, M. Shimada, S. Sarayama, H. Iwata, and F. J. Disalvo: J. Cryst. Growth **266** (2004) 461.
8) R. Dwiliński, R. Doradziński, J. Garczyński, L. P. Sierzputowski, A. Puchalski, Y. Kanbara, K. Yagi, H. Minakuchi, and H. Hayashi: J. Cryst. Growth **310** (2008) 3911.
9) C. Hemmingsson, P. P. Paskov, G. Pozina, M. Heuken, B. Schineller, and B. Monemar: J. Cryst. Growth **300** (2007) 32.
10) K. Motoki, T. Okahisa, N. Matsumoto, M. Matsushima, H. Kimura, H. Kasai, K. Takemoto, K. Uematsu, T. Hirano, M. Nakayama, S. Nakahata, M. Ueno, D. Hara, Y. Kumagai, A. Koukitu, and H. Seki: Jpn. J. Appl. Phys. **40** (2001) L140.
11) Ch. Hennig, E. Richter, M. Weyers, and G. Trankle: J. Cryst. Growth **310**

© 2010 The Japan Society of Applied Physics

(2008) 911.
12) T. Paskova, V. Darakchieva, P. P. Paskov, U. Sodervall, and B. Monemar: J. Cryst. Growth **246** (2002) 207.
13) J. R. Grandusky, V. Jindal, N. Tripathi, F. Shahedipour-Sandvik, H. Lu, E. B. Kaminsky, and R. Melkote: J. Cryst. Growth **307** (2007) 309.
14) Y. Andre, A. Trassoudaine, J. Tourret, R. Cadoret, E. Gil, D. Castelluci, O. Aoude, and P. Disseix: J. Cryst. Growth **306** (2007) 86.
15) K. Hiramatsu, T. Detchprohm, and I. Akasaki: Jpn. J. Appl. Phys. **32** (1993) 1528.
16) C. C. Tsai, C. S. Chang, and T. Y. Chen: Appl. Phys. Lett. **80** (2002) 3718.
17) B. Łucznik, B. Pastuszka, I. Grzegory, M. Bockowski, G. Kamler, E. Litwin-Staszewska, and S. Porowski: J. Cryst. Growth **281** (2005) 38.
18) V. Darakchieva, T. Paskova, P. P. Paskov, B. Monemar, N. Ashkenov, and M. Schubert: Phys. Status Solidi A **195** (2003) 516.
19) H. H. Huang, K. M. Chen, L. W. Tu, T. L. Chu, P. L. Wu, H. W. Yu, C. H. Chiang, and W. I. Lee: Jpn. J. Appl. Phys. **47** (2008) 8394.
20) D. Gogova, C. Hemmingsson, B. Monemar, E. Talik, M. Kruczek, F. Tuomisto, and K. Saarinen: J. Phys. D **38** (2005) 2332.
21) A. A. Porporati, Y. Tanaka, A. Matsutani, W. Zhu, and G. Pezzotti: J. Appl. Phys. **100** (2006) 083515.
22) C. Kisielowski, J. Kruger, S. Ruvimov, T. Suski, J. W. Ager III, E. Jones, Z. Liliental-Weber, M. Rubin, E. R. Weber, M. D. Bremser, and R. F. Davis: Phys. Rev. B **54** (1996) 17745.
23) D. C. Oh, S. W. Lee, H. Goto, S. H. Park, I. H. Im, T. Hanada, M. W. Cho, and T. Yao: Appl. Phys. Lett. **91** (2007) 132112.
24) M. A. Reshchikov and H. Morkoç: J. Appl. Phys. **97** (2005) 061301.
25) A. Kasic, D. Gogova, H. Larsson, C. Hemmingsson, I. Ivanov, B. Monemar, C. Bundesmann, and M. Schubert: Phys. Status Solidi A **201** (2004) 2773.
26) T. B. Wei, P. Ma, R. F. Duan, J. X. Wang, J. M. Li, and Y. P. Zeng: Chin. Phys. Lett. **24** (2007) 822.
27) L. Lu, Z. Y. Gao, B. Shen, F. J. Xu, S. Huang, Z. L. Miao, Y. Hao, Z. J. Yang, G. Y. Zhang, X. P. Zhang, J. Xu, and D. P. Yu: J. Appl. Phys. **104** (2008) 123525.
28) M. J. Kappers, R. Datta, R. A. Oliver, F. D. G. Rayment, M. E. Vickers, and C. J. Humphreys: J. Cryst. Growth **300** (2007) 70.

© 2010 The Japan Society of Applied Physics